Catena 227 (2023) 107123

Contents lists available at ScienceDirect

Catena

journal homepage: www.elsevier.com/locate/catena

The longest tree-ring based chronology of mass movements in Central Europe and their meteorological triggers

Karel Šilhán [a,*], Rudolf Brázdil [b,c], Pavel Zahradníček [c,d], Tomáš Pánek [a]

[a] Department of Physical Geography and Geoecology, University of Ostrava, Chittussiho 10, Ostrava 710 00, Czech Republic
[b] Institute of Geography, Masaryk University, Kotlářská 2, 611 37 Brno, Czech Republic
[c] Global Change Research Institute, Czech Academy of Sciences, Bělidla 986/4a, 603 00 Brno, Czech Republic
[d] Czech Hydrometeorological Institute, Brno Regional Office, Kroftova 43, 616 67 Brno, Czech Republic

ARTICLE INFO

Keywords:
Dendrogeomorphology
Landslide
Meteorological triggers
Long chronology

ABSTRACT

Knowledge of meteorological triggers of mass movements is crucial for determining the degree of hazards, but also for predicting their occurrence. Dendrogeomorphic methods (tree-ring based) have repeatedly provided data on historical landslide activity as a basis for detailed trigger analysis. However, the construction of long dendrogeomorphic chronologies encounters limits in the sensitivity of growth disturbances in trees as well as their age dependence. Moreover, accurate meteorological instrumental data usually do not cover the entire length of long tree-ring based chronologies of landslide movements. To resolve these uncertainties, this study has compiled the longest tree-ring-based chronology of mass movements in Central Europe for Mt. Kněhyně in Outer Western Carpathians, spanning more than a quarter of a millennium and based on 228 tree-ring series of disturbed individuals of Norway spruce (*Picea abies* (L.) Karst.). The resulting chronology is a combination of two sub-chronologies that we constructed from different tree growth disturbances (reaction wood and tree-ring eccentricity), combining the advantages of both approaches. To identify potential meteorological triggers, we combined instrumental data from the nearest meteorological station together with reconstructed data from the wider landslide study area and documentary records. This gave us a uniquely long overlap of the two datasets across the full length of the mass movement chronology, allowing for more robust results compared to significantly shorter overlays. The studied mass movements followed up to three years of above-mean precipitation and were immediately triggered by short (several days) precipitation extremes. Snowmelt lasting several days to weeks in selected cases further modified this pattern.

1. Introduction

The occurrence of landslides, as one of the most dangerous natural hazards, is often associated with the occurrence of extreme hydrometeorological events (Chitu et al., 2017; Jakob et al., 2006; Xian et al., 2022). Therefore, the relationship between landslide occurrence and these extreme events is one of the most frequently investigated aspects in comprehensive landslide research (Notti et al., 2021). Indeed, a detailed analysis of the triggering factors of landslides can be used to predict their general activity in the coming decades thanks to climate prediction models (Khan et al., 2022). This aspect becomes even more important today in the context of ongoing global climate change (Stoffel and Beniston, 2006). However, in order to precisely define the relationship between trigger parameters and the occurrence of landslide movement, the most accurate chronological information on landslide events is needed, as well as appropriate meteorological data. Unfortunately, archival records of landslide events are generally very limited and usually even completely missing (Raška et al., 2015). This is especially true for landslides in remote areas.

The solution in this case is to use absolute dating methods, of which the dendrogeomorphic approach is currently considered to be the most precise (provided that trees capable of forming annual tree rings are present). The normal range of tree-ring based methods is tens (Wistuba et al., 2013) to the first hundreds of years (Shroder, 1978; Šilhán et al., 2012). However, the longest tree-ring based chronology constructed to date reaches up to a thousand years (Zhang et al., 2019). The precision of this approach is typically on the order of a year, but it is possible to achieve up to seasonal resolution (Lopez Saez et al., 2012a, 2012b;

* Corresponding author.
E-mail address: karel.silhan@osu.cz (K. Šilhán).

https://doi.org/10.1016/j.catena.2023.107123
Received 8 December 2022; Received in revised form 22 March 2023; Accepted 28 March 2023
Available online 5 April 2023
0341-8162/

Stefanini, 2004). The method is based on dendrochronological dating of the growth response of trees to mass movements (Shroder, 1978). This principle makes it possible to obtain both the chronology (Shroder, 1978; Zhang et al., 2019) and the spatiality (Lopez Saez et al., 2012a, 2012b) of landslide events. However, the data are often used as a basis for the analysis of triggers (Wistuba et al., 2021b), both short-term (Šilhán et al., 2013) and long-term (Wistuba et al., 2021a) above-mean precipitation, or spring snowmelt (Šilhán, 2012).

Unfortunately, to maximize the use of long tree-ring based chronologies for trigger analysis, the limiting factor tends to be the length of the meteorological data series and its overlap with the landslide chronology. Most of the longest series of landslide movements and meteorological data compared do not use the full length of the tree-ring chronology. For example, the longest overlap with instrumental data to date was presented by Šilhán et al. (2012) (132 years), but still more than half of the reconstructed landslide chronology (307 years) remained unused for meteorological trigger analysis. Other similar examples include studies by Shroder (1978) or Fantucci and Sorriso-Valvo (1999). However, Zhang et al. (2019) used dendroclimatically reconstructed precipitation data as a replacement for instrumental data. Another solution may be to use meteorological data from the wider region of the study site or to use documentary records of the occurrence of hydrometeorological extremes (Brázdil et al., 2005). However, this data source has not yet been used for comparison with tree-ring chronology of landslide movements. In doing so, this alternative source of meteorological data would allow a significant extension of the overlap period, which should lead to an increase in the robustness of the results of the analysis of landslide triggers.

Identification of a range of tree growth disturbances (e.g., reaction wood, abrupt growth changes, eccentric growth, or anatomical changes in the tree rings; Šilhán, 2020; Stoffel and Corona, 2014) or a combination of these is used to reconstruct the landslide event. The stem tilting is a dominant effect of slope movement on tree growth, to which trees respond by forming reaction wood (Westing, 1965) or eccentric growth (Braam et al., 1987). Each of these responses has its own specifics and differences. Reaction wood is generally less sensitive to minor movements due to creep and so may not experience small slide movements on the order of tenths of mm. In contrast, eccentric growth is more sensitive, and can record very small landslide movements as well as creep movements (Fabiánová et al., 2021). Analysis of the spatial distribution of growth disturbances can be used to distinguish between the two types of movements (Lopez Saez et al., 2012a, 2012b). The combination of both types of growth disturbances seems to be optimal for reconstructing landslide movements also because both are subject to different age-dependent tree sensitivity. In particular, younger trees respond through reaction wood, whereas older trees are more likely to respond through eccentric growth (Šilhán, 2021a). The use of either type of growth disturbance has occasionally been used in the past to construct two distinct chronologies (Cockburn et al., 2016; Pánek et al., 2011a, 2011b; Šilhán and Stoffel, 2015) or both reactions have been equivalently included in the list of landslide signals used to construct the resulting chronology (Bollati et al., 2012; Corominas and Moya, 1999; Pawlik et al., 2013). However, the construction of separate sub-chronologies (including spatial testing of growth disturbance) and their subsequent combination has not yet been implemented. Meanwhile, the aforementioned procedure could provide a more robust data source for the analysis of landslide triggers.

Based on the above challenges, the main objective of this study is to construct a robust chronology of slope movements using a unique combination of the two most common types of tree growth responses to landslide movements. Subsequently, this chronology at its maximum length will be subjected to an analysis of causal meteorological triggers, with the overall overlay of the mass movement chronology provided, in a dendrogeomorphic study, by a unique combination of instrumental data, data from the wider region of the study locality, and documentary data for the earliest period of the reconstructed chronology. This should result in a unique overlap of the two time series of several centuries in duration, giving a more objective picture of the linkage of mass movements and their triggers.

2. Study area

For the purpose of this study, a landslide was selected on the eastern slope of Mt. Kněhyně (49.495°N; 18.315°E; 1257 m a.s.l.) in the Moravskoslezské Beskydy Mts. (Outer Western Carpathians; Fig. 1). The region of the study site has a nappe structure involving thrusts and folds of Miocene age. Geologically, it is characterized by a flysch structure with alternating layers of rigid sandstones and conglomerates with mechanically weak claystones and siltstones of late Cretaceous age (Menčík et al., 1983). The flysch beds are slightly (10–20°) inclined towards the S–SE. The Moravskoslezské Beskydy Mts. are characterized by dissected mountain ridges exceeding up to 1200 m a.s.l., which are separated by deep valleys. The slopes are very steep (up to 35°), though the mountains were not glaciated during the Pleistocene. The only remnants of the cold Pleistocene periods are stony colluvia covering the slopes (Pawelec, 2006). Mean annual precipitation reaches 1390 mm (the 1961–2000 period) at the highest point of the mountain range (Mt. Lysá hora; 1322 m a.s.l.; approx. 11 km from the study site). During the summer season, precipitation often takes the form of downpours during thunderstorms. The mean annual temperature on the Mt. Lysá hora is 2.6 °C and snow cover lies on average about 170 days per year (Tolasz et al., 2007). The wider region of the study landslide can thus be described as one of the wettest areas in Central Europe. The combination of humid climate, geology, anisotropy of flysch and high local relief is the main reason for the very frequent occurrence of mass movements of different types (Pánek et al., 2019). Especially rotational and translational landslides (Pánek et al., 2011a, 2011b; Šilhán et al., 2013), with some rock avalanches (Pánek et al., 2009), rockfalls (Brázdil et al., 2012b; Šilhán et al., 2011) and debris flows (Šilhán, 2023) are present. Currently, the vegetation composition of the forests is represented by European beech (*Fagus sylvatica* L.), sycamore maple (*Acer pseudoplatanus* L.), Norway spruce (*Picea abies* (L.) Karst.), European larch (*Larix decidua* Mill.) or white fir (*Abies alba* Mill.). In the 1970s, however, the slopes were partially deforested due to tree death caused by air pollution from the Ostrava industrial area to the north. The original forests are preserved only in limited areas and the largest refugium of the oldest *P. abies* individuals is located on the top of Mt. Kněhyně, which is also affected by the studied landslide. Thus, the combination of the presence of a large landslide and the oldest *P. abies* individuals provides ideal conditions for the implementation of this study.

The studied landslide affects the eastern and southern slope of the of Mt. Kněhyně (Fig. 1). The upper limit of the landslide is located just below the summit and terminates at the bottom of the Čeladenka River valley. The total elevation of the landslide thus reaches up to 700 m and the length is about 1900 m. The mass movement has the character of a deep-seated rotational-translational landslide, which is partly predisposed by bedding planes with tension cracks and trenches in its upper part. The upper part of the landslide has the character of stepped blocks, which turn into toe with compression features downslope. The part of the landslide area below the summit of Mt. Kněhyně with a southern orientation has the morphological character of shallower movements (Fig. 1B). Crevice-type caves occur in the upper and middle part of the landslide (Wagner et al., 1990). Based on geophysical measurements across the upper part of the landslide (Lenart et al., 2014) by electrical resistivity tomography (ERT), individual flysch beds and incipient sliding surface of landslide are evident at a depth of ~ 30 to 35 m. The shallow colluvium covering the landslide blocks and filling the trenches between them reaches a maximum depth of about 5 m (Fig. 1C). The presence of snow avalanches has never been observed at the study site (Kříž, 1995), and therefore the influence of this process (which can induce the same growth responses in disturbed trees as landslides) can be ruled out.

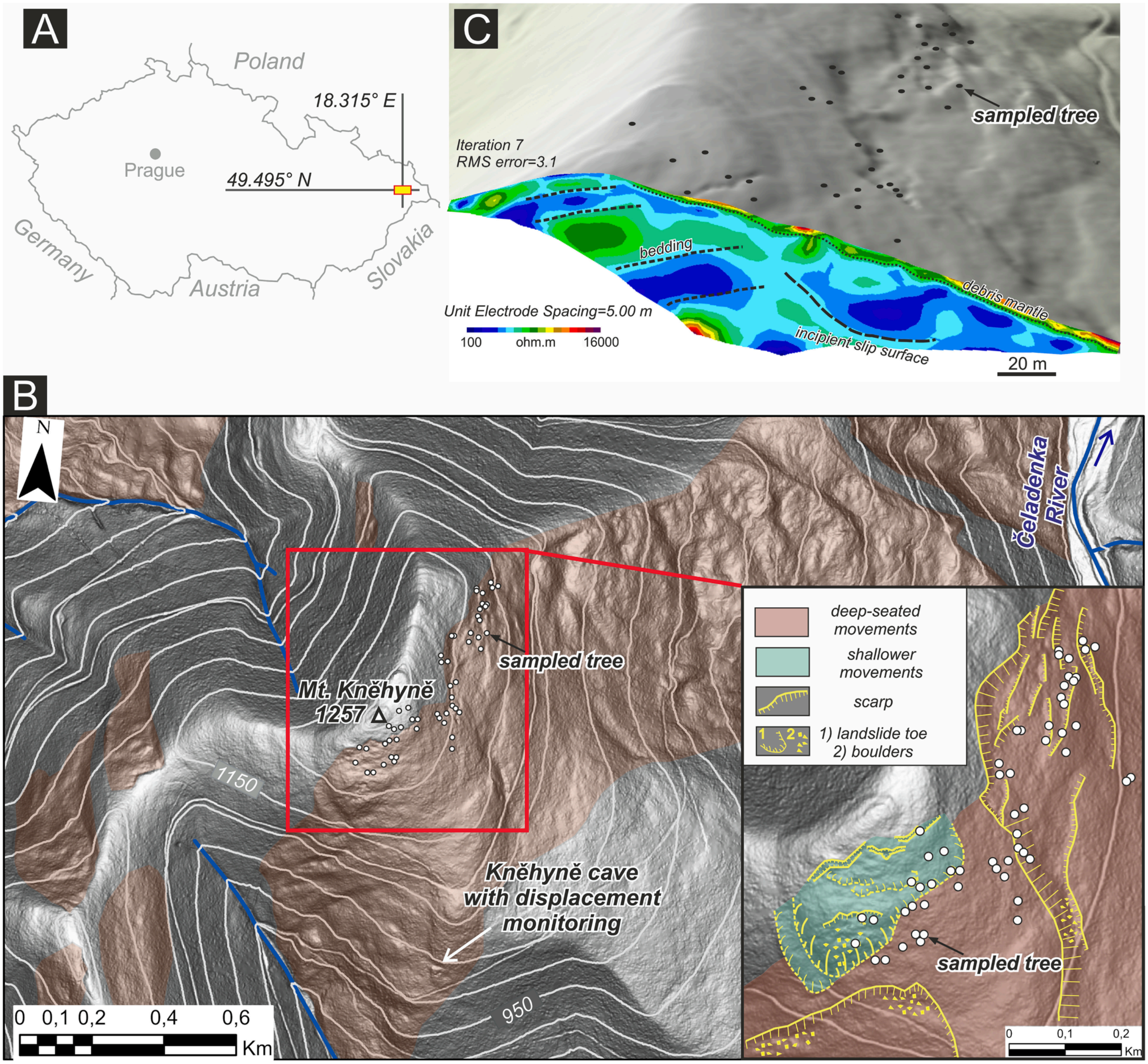

Fig. 1. Position of the studied locality. A - position within the Czech Republic, B - Hillshade of the Mt. Kněhyně ridge with indication of the landslide area (brown colour) and an inserted geomorphological map of the area selected for dendrogeomorphological sampling, C - geophysical (ERT) profile across the studied part of the landslide (adapted after Lenart et al., 2014).

3. Data and methods

3.1. Fieldwork

The studied landslide was first mapped in detail geomorphically (approximately 1:500) on the basis of LiDAR data and orthophoto using GNSS equipment. The mapping focused on the basic morphological features of the landslide area (main scarp, individual landslide blocks, tension cracks, minor scarps, zones with shallow movements). For the dendrogeomorphic reconstruction of slope movements, trees that showed their growth affected by slope movement (tilted stems) were selected and sampled. The position of each selected tree was recorded using a GNSS receiver on a geomorphic map. Due to the geomorphology of the landslide, trees were sampled only in the upper part of the landslide area (area of partial landslide blocks) where the dominance of landslide movements can be expected compared to the middle and lower part of the slope, where due to the high slope gradient and the assumed thickness of the colluvial mantle there would be a risk of noise due to the presence of creep movements. Moreover, only this part of the landslide is covered by an old (>100 years) forest consisting of *P. abies*. Each tree was sampled using a Pressler increment borer (maximum length: 50 cm; diameter: approximately 0.5 cm) at the height of maximum stem bend (Braam et al., 1987). Four increment cores were taken from each tree (one from the lower side of the stem, one from the opposite side of the stem, and two orthogonal to the first two). Reference trees growing in the same microclimatic conditions but outside the landslide area were also sampled to identify any false or missing tree rings.

3.2. Laboratory processing and compilation of slope movement chronology

All samples (disturbed and reference) were processed using standard dendrogeomorphic methodology (Šilhán, 2020; Stoffel and Bollschweiler, 2008). Increment cores were air-dried, glued to woody supports and sanded to make all tree rings clearly visible. Tree rings were then counted and their widths were measured using the dendrochronological TimeTable and PAST4 software (V.I.A.S., 2005) with an accuracy of 0.01 mm. The disturbed samples were then visually cross-dated against a reference chronology that was constructed in the Arstan program (Cook, 1983). The accuracy of the dating was independently verified statistically in the Cofecha (Holmes, 1983).

The construction of the resulting chronology of mass movements was based on a combination of two sub-chronologies that were constructed based on two different tree growth responses. The first chronology reflected the temporal occurrence of reaction (compression) wood, which is the growth anatomical response to tree stem tilting (Westing, 1965). This growth disturbance was identified by visual inspection of the disturbed surface of disturbed specimens, where it showed its brown-reddish colour due to the thick cell walls of the compression wood (Fig. 2). The second chronology was based on the sudden change in tree-ring eccentricity (e), which was calculated using the formula $e = (a + c)/(a–c)$, where a is the tree-ring width on the underside of the tilted stem and c is the tree-ring width on the lateral side of the stem (Braam et al., 1987). The calculated e values were then converted to weights ($e < 0.25$ = weight 0; $0.25 < e < 0.5$ = weight 1; $e \geq 0.5$ = weight 2). The timing of the slope movement was identified according to the methodology of Šilhán et al., (2014) as a sudden change in tree-ring eccentricity, which was manifested by a specific pattern of the weights (Fig. 2; e.g., 0022 = very strong signal).

Non-geomorphological influences (e.g. prevailing wind direction or canopy snow load) can also cause changes in tree-ring eccentricity and reaction wood formation. However, these influences are more areal than localised mass movements, and hence reference trees growing close to the study site are also affected. Therefore, to exclude the influence of these factors on the formation of the growth disturbances of interest, samples from disturbed trees were carefully compared with samples from reference trees. Only growth disturbances not contained in the reference trees were considered to be the result of mass movements. Because very young trees may also be sensitive to non-geomorphic influences (e.g., snow creep) that can induce the same growth responses as mass movements, the first decade of life of all trees was excluded from the analysis (Stoffel and Bollschweiler, 2008).

The two partial chronologies of mass movements were subsequently constructed in the same way. Individual growth disturbances were summarized into years and the identification of a mass movement event was based on the calculation of a standard event-response (I_t) index (Shroder, 1978), which represents the percentage of trees with a growth disturbance in a particular year out of all sampled trees that were alive in that year. The threshold for defining a slope movement event was set adaptively by the total number of sampled trees (Stoffel et al., 2013) at 5 % (for sample sizes above 30 trees) and 7.5 % (for sample sizes below 30 trees). In addition to the I_t index threshold, at least two trees had to always exhibit growth disturbance (Corona et al., 2014). In addition, spatial patterns of disturbed trees were tested by calculating the Moran index (Moran, 1950) in ArcMap software to distinguish events with a dispersed or more clustered spatial pattern (Lopez Saez et al., 2012b). The resulting chronology of mass movements for input to the meteorological trigger analysis consisted of combining mass movement years from both sub-chronologies.

3.3. Meteorological data

None meteorological measurements are available for Mt. Kněhyně ridge, but using measurements of meteorological stations from surroundings (the station network of the Czech Hydrometeorological Institute) was possible to create maps of spatial distribution of annual precipitation totals for the 1881–2020 period and reconstruct a related precipitation time series for site of Mt. Kněhyně. From this data were compiled series consisting of one-year, two-year and three-year precipitation totals. To characterise meteorological variables on the daily level, meteorological observations of the nearby Mt. Lysá hora station were used. This station is located in a distance of c. 11 km from Mt. Kněhyně in slightly higher position (by 65 m). Measurements at this station are available from 1898 with gaps (none or incomplete measurements in 1940–1946 and 1954) until present time. Daily records of Mt. Lysá hora were used to create series of maximum 3-day, 5-day and

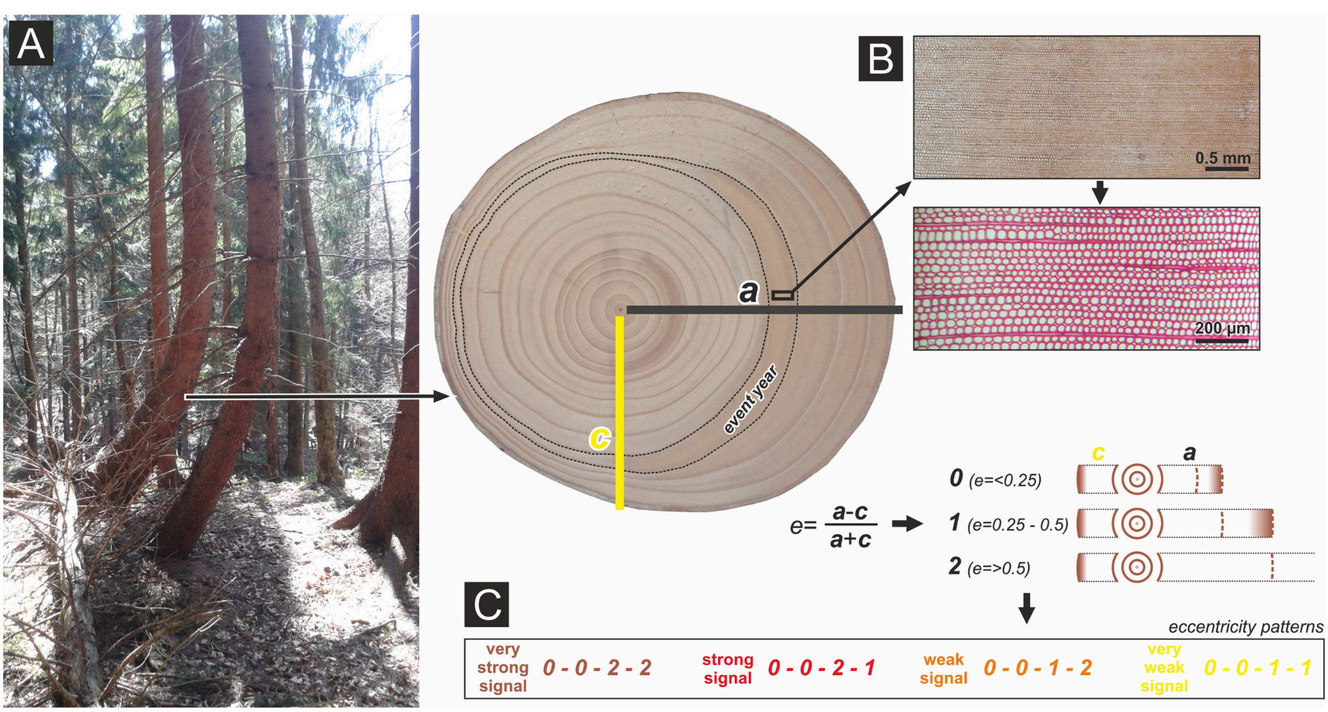

Fig. 2. Methodological approaches for geomorphic signal detection in tree-ring series of disturbed trees. A - Bent tree stems as a consequence of their leaning due to mass movements, B - macroscopic and microscopic appearance of the reaction wood, C - principle of geomorphic signal extraction based on changes in tree-ring eccentricity (assigning weights to tree-ring eccentricity values and tracking their temporal pattern).

10-day precipitation totals, maximum daily snow depths and maximum 7-day and 14-day snow melting. To characterise the mass movement years before 1881, we may use only instrumental or documentary meteorological data to be not directly related to the Mt. Kněhyně region.

Because of no information of real occurrence of landslides and time of their occurrence in potentially delimited years, we selected different meteorological variables as a potential triggers of mass movement events. To characterise potential impacts of wetter spells in detected 27 mass movement years on Mt. Kněhyně, we considered annual precipitation totals in the year of mass movement (n) and sums of totals for the year of mass movement with preceding one (n–1) and two preceding (n–2) years. Box-plots (median, upper and lower quartile, maximum and minimum) were used to compare these totals for the mass movement years with the rest of years (non-landslide) for the Mt. Kněhyně series. Because high daily precipitation totals may play the role of immediately triggering mechanism, we considered also 3-day, 5-day and 10-day precipitation totals comparing their box-plots for selected mass movement years with those remaining, based on related series of the Mt. Lysá hora station in the 1898–2020 period. Among snow characteristics, which may also influence a landslide origin, we used maximum snow depths and maximum 7-day and 14-day snow melting in selected mass movement years expressed by box-plots were compared with those in remaining years using related series of the Mt. Lysá hora station in the 1898–2020 period. A detailed overview of the overlap of single sources of meteorological data with the resulting chronology of reconstructed mass movements is given in Fig. 3.

4. Results

4.1. Analyzed trees and dated growth disturbances

A total of 57 disturbed trees (*P. abies*; 228 increment cores) covering the upper part of the study Mt. Kněhyně landslide were sampled (Fig. 1). The mean age of the sampled trees was 145.1 years (standard deviation; stdev: 51.6 years), with the oldest tree being 296 years old and the youngest being 25 years old. There were 23 trees older than 150 years and five trees older than 250 years. Onset of reaction wood was identified in 52 cases in the tree-ring series. It contributed to the final identification of mass movement events in 40 cases (76.9 %). Analysis of abrupt changes in tree-ring eccentricity revealed the presence of 284 growth disturbances. Of this number, 156 (54.9 %) were involved in the identification of mass movement. Of all the tree-ring eccentricity intensities, very weak (75.0 %) dominated, while very strong was the least represented (4.5 %). The relative proportion of sudden changes in tree-ring eccentricity in mass movement years and other years is shown in Fig. 4A. The intensity of growth responses was generally significantly higher (p-value from Mann-Whitney test < 0.01) in mass movement years compared to other years (noise) (Fig. 4A).

4.2. Chronology of mass movements

A partial chronology of mass movements based on the analysis of the occurrence of reaction wood revealed 13 mass movement years. In contrast, a partial chronology constructed based on changes in tree-ring eccentricity revealed 30 mass movement years (Fig. 5). The intensity of change in these growth disturbances showed no dependence with event-responses (I_t) index values in mass movement years or other years (Fig. 4B). Synchronous events from both subchronologies occurred in eight cases, representing 61.5 % of events constructed from reaction wood and 26.6 % of events constructed from tree-ring eccentricity (Fig. 5A). Combining the two subchronologies thus produced a final chronology of slope movements that contains a total of 35 mass movement years since 1784, when the oldest event was reconstructed (Fig. 5B). However, the total length of the chronology covered by at least five trees reaches a length of 252 years (1759–2011). Moran index values for mass movement years averaged 0.076 (stdev: 0.102) with a maximum of 0.257 for the subchronology based on reaction wood detection and averaged 0.061 (stdev: 0.095) with a maximum of 0.345 for the subchronology based on tree-ring eccentricity (Fig. 6).

4.3. Potential meteorological triggers of slope movements

All three analysed categories of annual precipitation totals (n, n + (n − 1), and n + (n − 2)) show systematically higher values in five box-plot characteristics for the group of 27 detected mass movement years compared to those remaining other years (Fig. 7). Moreover, according to *t*-test, mean precipitation totals in the group of mass movement years are statistically significantly higher than those in the group of remaining other years ($p < 0.01$) in all three categories. Analogously as in the preceding case of annual totals, also 3-day, 5-day and 10-day precipitation totals show significantly higher values for box plots in the group of mass movement years compared to box plots of remaining other years (Fig. 8). Differences in corresponding means are also statistically significant ($p < 0.01$).

All three snow characteristics show generally high variability in other years indicating that the highest values of snow depth and snowmelt were not always followed by mass movements event. Although the absolute minimum, lower quartile and median of maximum snow depths are higher for mass movement years, the difference in means of both landslide and non-landslide datasets were not

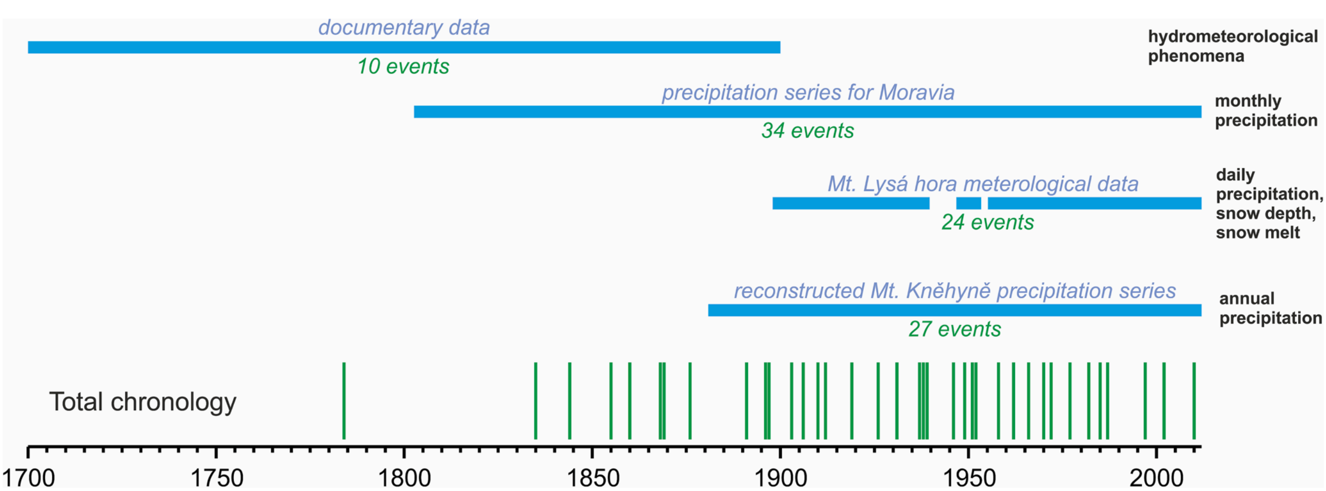

Fig. 3. Temporal overlap of different meteorological data sources with the resulting compiled chronology of mass movements, including the events covered by each data source.

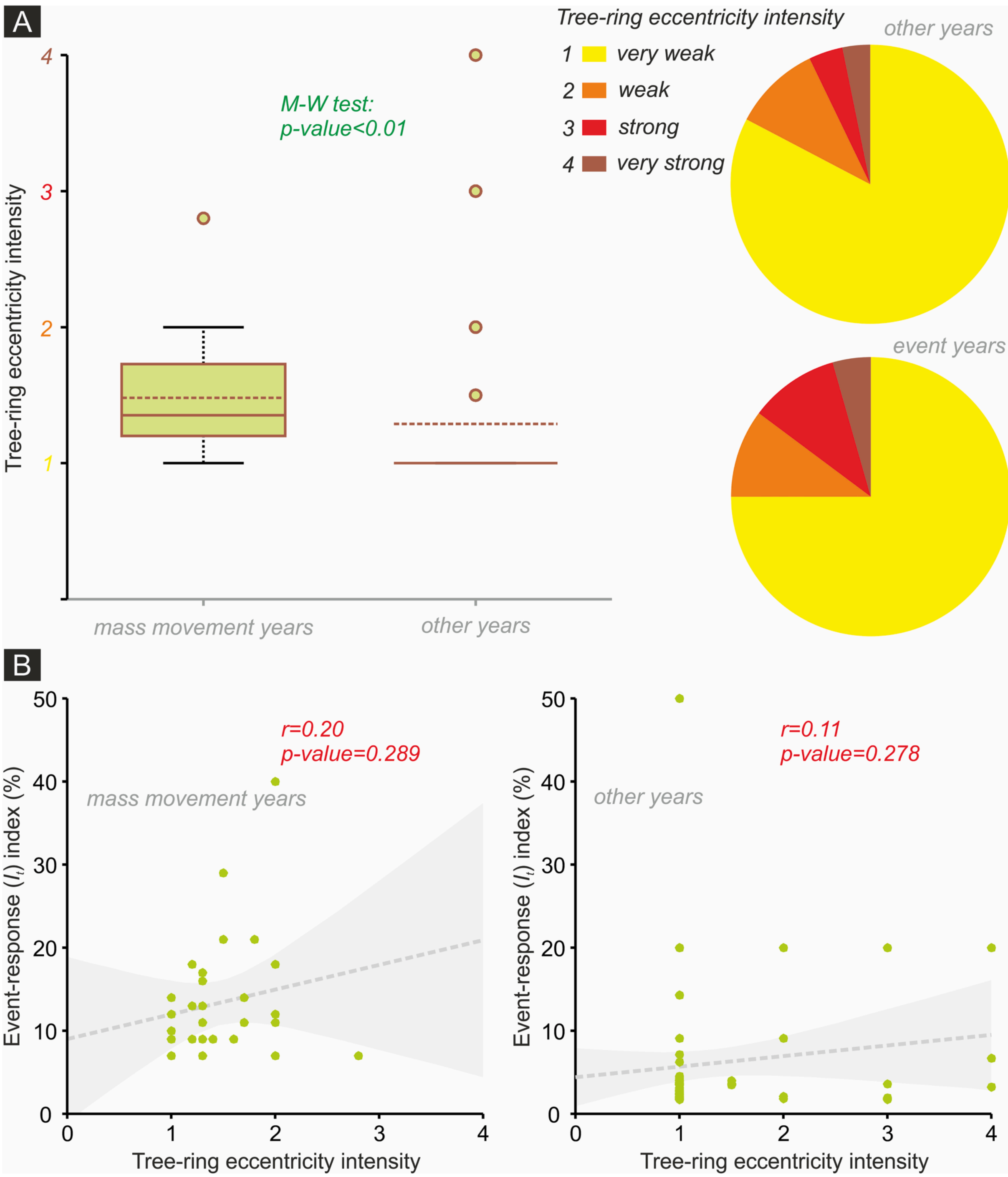

Fig. 4. Intensity tree-ring eccentricity in mass movement years and other years. A - Proportions and overall representation of geomorphic signal intensities based on the magnitude of tree-ring eccentricity change, B - relationship between the magnitude of the event-response index and the magnitude of tree-ring eccentricity change.

statistically significant (Fig. 9). Concerning of 7-day and 14-day snow melting, despite higher values of minimum, lower quartile, median and upper quartile values in mass movement years, statistically significant differences in corresponding means of both datasets were found only for 7-day snow melting ($p < 0.05$). These results indicate much smaller potential effect of snow cover on the mass movement origin compared to preceding precipitation variables.

In order to characterise in which potential mass movement years the meteorological conditions were more or less favourable for the mass movement origin, all 23 such years between 1903 and 2010 (except 1946) were ordered for each meteorological variable from the highest to the lowest values. Separately were considered three variables in annual precipitation totals and three variables in daily precipitation totals. The resulting orders of the given year in these two groups were then added to obtain precipitation scores with potential values between 2 and 46. The same approach was applied for maximum snow depths and snow melting (for 7-day and 14-day taken together) to obtain comparable snow scores with potential values between 2 and 46 for mass movement years. Applying this approach, each potential mass movement year is now characterised by precipitation and snow scores. These values were

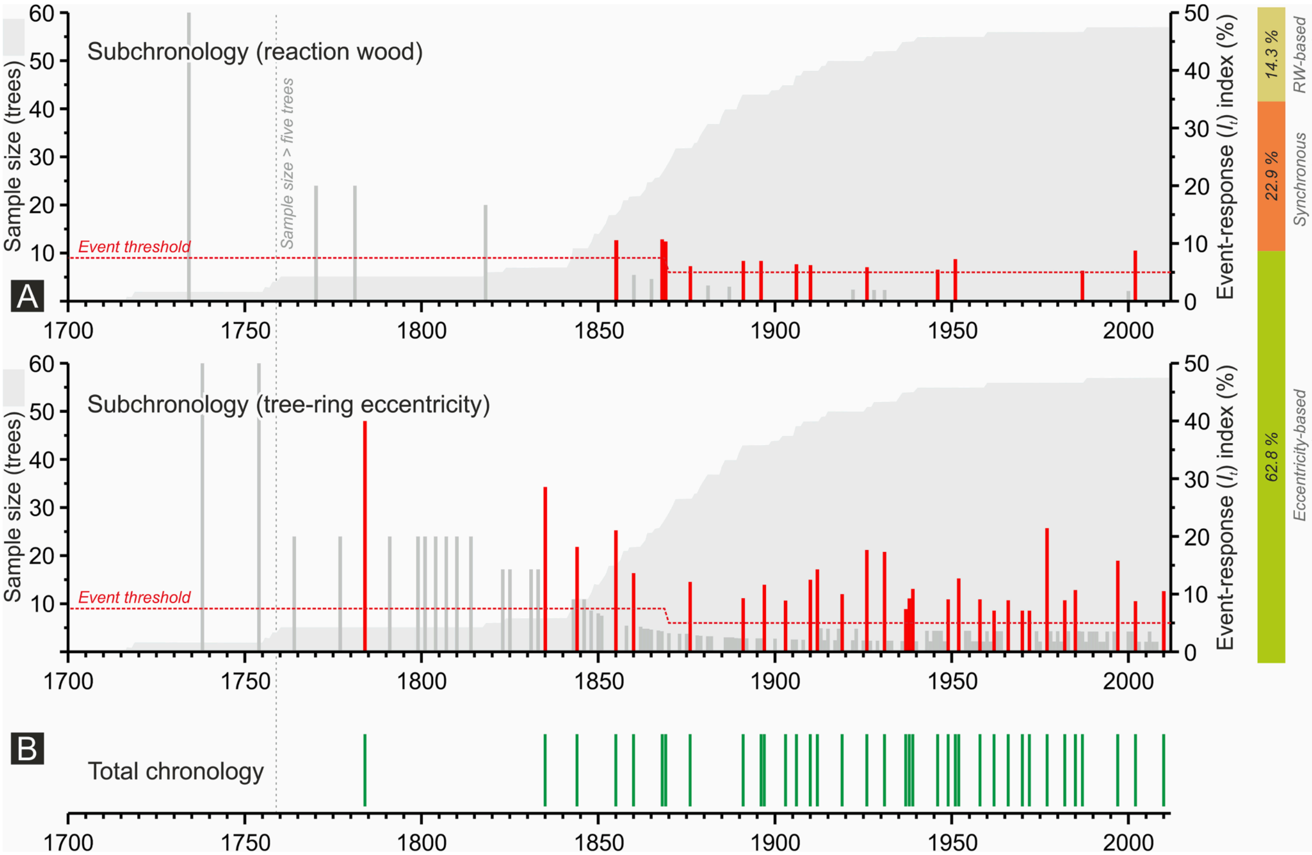

Fig. 5. Chronology of mass movements. A - subchronologies of mass movements compiled on the basis of identification of reaction wood and according to changes in tree-ring eccentricity values (grey column - years when the minimum I_t index value was not reached or less than two trees were disturbed; red column - mass movement event meeting the I_t index threshold and minimum number of disturbed trees), B - overall chronology of mass movements compiled as a compendium of two sub-chronologies. (For interpretation of the references to colour in this figure legend, the reader is referred to the web version of this article.)

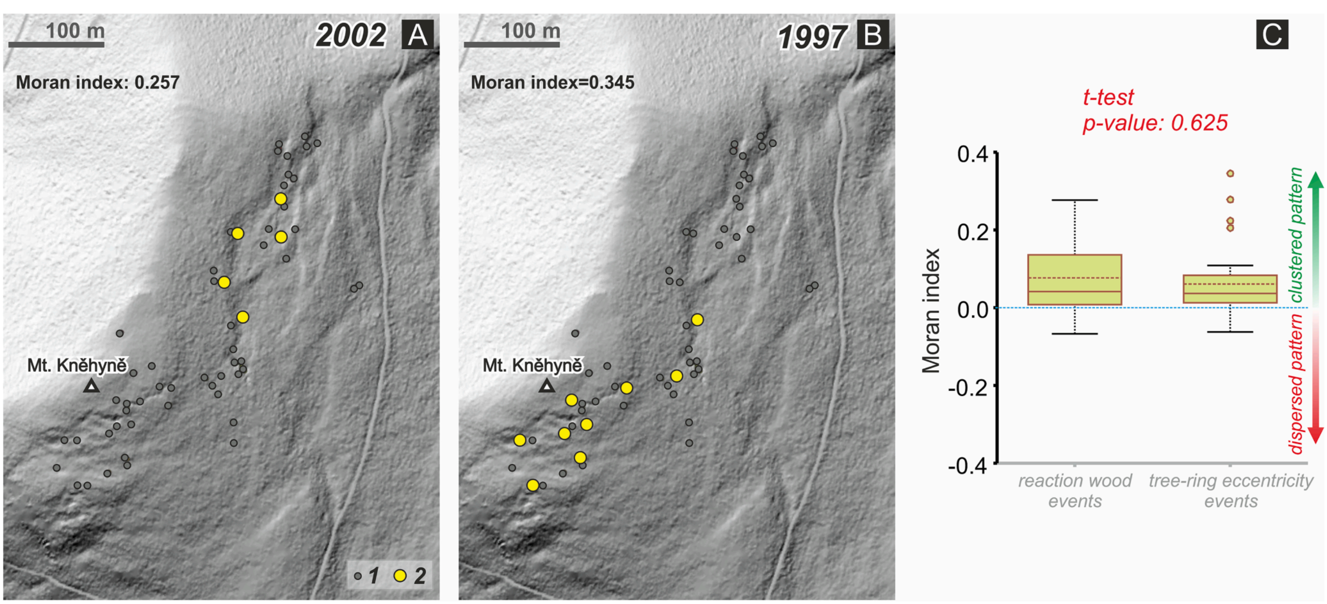

Fig. 6. Spatial distribution of tree-ring mass movement signals expressed using the Moran index. A - spatial distribution of disturbed trees in the mass movement year with the highest Moran index value in the subchronology constructed according to the identification of the reaction wood (1 - sampled tree, 2 - tree with growth disturbance in a given year), B - spatial distribution of disturbed trees in the year with the highest Moran index value in the subchronology constructed according to changes in the tree-ring eccentricity value, C - summary of all Moran index values in mass movement years from both subchronologies.

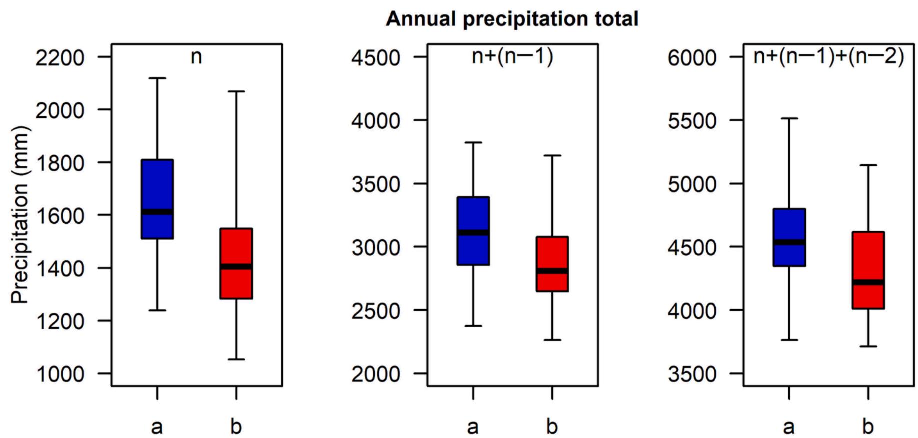

Fig. 7. Box-plots (median, upper and lower quartile, maximum and minimum) of one-year (n), two-year (n + (n − 1)) and three-year (n + (n − 1) + (n − 2)) precipitation totals in 27 selected mass movement years (a) compared to remaining (other) years (b) for the Mt. Kněhyně 1881–2020 precipitation series.

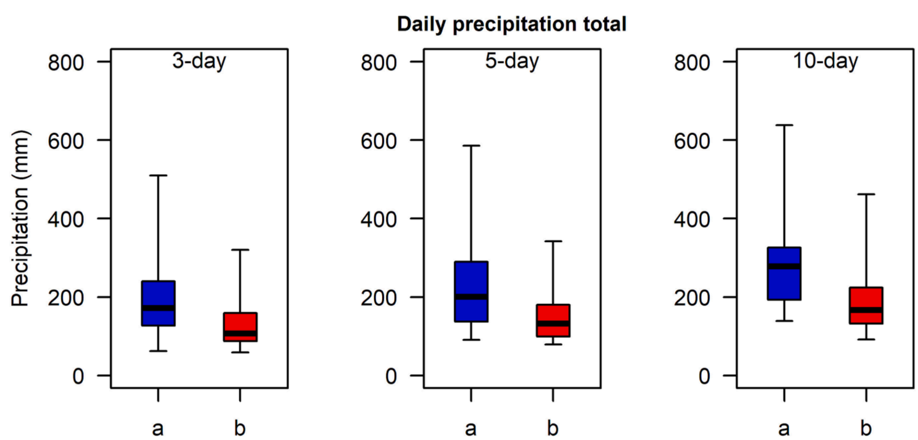

Fig. 8. Box-plots (median, upper and lower quartile, maximum and minimum) of 3-day, 5-day and 10-day precipitation totals in 24 selected mass movement years (a) and in 93 remaining (other) years (b) for the Mt. Lysá hora 1898–2020 precipitation series.

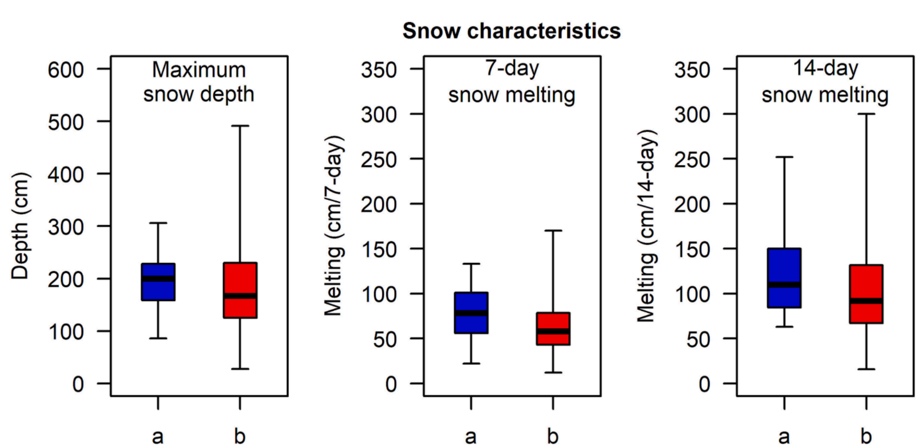

Fig. 9. Box-plots (median, upper and lower quartile, maximum and minimum) of maximum snow depths and maximum 7-day and 14-day snow melting in 24 selected mass movement years (a) and in 93 remaining (other) years (b) for the Mt. Lysá hora 1898–2020 precipitation series.

included in the graph and complemented by lower and upper quartile separately for precipitation and snow scores (Fig. 10). It allows to distinguish mass movement years with dominant precipitation effects (1903, 1912, 1926, 1966, 1972, 1997, 2002, 2010) with those with rich snow patterns and sudden snowmelt that could enhance the effects of high annual and daily precipitation totals (1906, 1919, 1939, 1952, 1958, 1962, 1982).

As for the other selected mass movement years being out of 23 described in detail by precipitation and snow scores (see Figs. 3 and 10), their meteorological patterns with respect to mass movement origin can be described less exactly. If we take in account one-year, two-year and three-year precipitation totals for Mt. Kněhyně for 27 mass movement years in 1881–2020 (see Fig. 7), precipitation triggers in this context were less pronounced for 1891 (17th in the order from 26), 1946

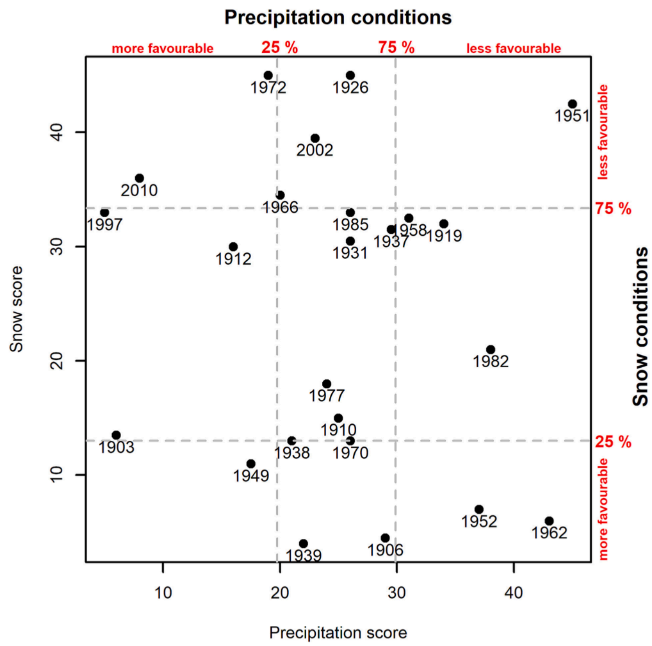

Fig. 10. Relatively more favourable and less favourable precipitation and snow conditions for the landslide origin expressed by their scores for 23 selected mass movement years from 1903 to 2010 (without 1946 – missing meteorological data) and complemented by values of upper (75 %) and lower (25 %) quartiles of precipitation and snow scores.

(19th–20th) and 1897 (23rd). Despite the specific precipitation character of the Moravskoslezské Beskydy Mts. region, we may try to characterise precipitation patterns of nine selected mass movement years of the 19th century in the context of all 34 mass movement years based on the same approach using mean annual precipitation totals for Moravia available from 1803 until present (Brázdil et al., 2012a). As follows from Table 1, from the mass movement years of the 19th century, the 1897 year was even the 11th wettest and 1855 the 18th, while 1835 was the last 34th in the order of all detected mass movement years (1869 the 32nd–33rd and 1868 the 30th).

Concerning of the last detected slope movement year 1784, it is a year of extreme February–March floods in central Europe after very severe and snowy 1783/84 winter following the Lakagígar 1783 eruption in Iceland (Brázdil et al., 2010), but the summer 1784 was dry in the Czech Lands (Brázdil et al., 2017).

5. Discussion

The longest chronology of slope movements in Central Europe was compiled on the Mt. Kněhyně landslide (Outer Western Carpathians)

Table 1
Selected mass movement years of the 19th century and their characteristics (N – the precipitation order of the given year in the context of all 34 selected mass movement years for Moravia).

Year	N	Additional documentary data from the Czech Lands
1835	34th	The second dry year after 1834, bark beetle calamity.
1844	27th	Much snow, floods in May, rainy summer.
1855	18th	Floods from snowmelt, rainy summer, August flood on the Bečva River.
1860	24th	Much snow, snowmelt floods, July flood on the Opava River.
1868	30th	Early-March snowmelt flood in Bohemia.
1869	32nd–33rd	Late-November flood on the Bečva River.
1876	22nd–23rd	February–March snowmelt flood.
1891	22nd–23rd	Much snow, early-March snowmelt flood, rainy summer, July flood on the Odra River.
1897	11th	Large late-July floods.

over 252 years based on data from 228 tree-ring series of disturbed *P. abies* individuals. The resulting chronology was produced by a rare combination of the results of two partial dendrogeomorphic chronologies obtained by different meteorological approaches, thus combining the advantages of both. The observed years of mass movements were subsequently used as the basis for the analysis of meteorological triggers throughout the chronology. The result of this methodological approach is a complete overlaps of the entire tree-ring based chronology of mass movements with meteorological data in a unique and largest ever length covering more than a quarter of a millennium (cf. Table 2).

5.1. Dendrogeomorphic aspects of mass movement chronology

Dendrogeomorphic dating can detect almost any type of hillslope processes (Šilhán, 2021b) while the character of recorded movements may not directly reflect the morphological features of the studied site. For this reason, it is critically important to define what type of movement has been reconstructed at each study site (Stoffel and Bollschweiler, 2008). In this study, it is possible to define the type of mass movement based on indices consisting of the proportion of growth disturbances by which mass movement has been reconstructed (Šilhán et al., 2022a), the spatial pattern of disturbed trees (Lopez Saez et al., 2012b), and the geophysical ERT record. Based on the analogous parameters of these indications from the studies by Fabiánová et al. (2021) and Šilhán et al. (2022a, 2022b), the reconstructed mass movements appear to have the character of shallow to medium-deep sliding (within a few meters or at most the first tens of meters), affecting both the landslide blocks themselves and the colluvial mantle. The assumption that we have detected only the shallow surface movements is consistent with the data from the displacement monitoring of landslide movements, which has been implemented for a long time in a crevice-type cave located directly in the studied landslide at a depths of 25 and 57.5 m respectively (Stemberk et al., 2017). Extensional movements measured in this crevice are very low, ranging between 0.05 and 0.2 mm/yr, with higher values in the shallower position (Stemberk et al., 2017), which, together with our dendrogeomorphic data, clearly indicates a decreasing rate of movements towards the base of the landslide.

The different number of reconstructed slope movements in the two subchronologies reflects both the methodological approach itself (subjective identification of reaction wood vs. mathematical definition of the event by changes in tree-ring eccentricity) and the ability of trees to respond with appropriate growth responses to mass movements of different magnitudes (Šilhán, 2016). The approach based on changes in tree-ring eccentricity is generally considered to be more sensitive (Pawlik et al., 2013), but only for older trees (Šilhán and Stoffel, 2015). Moreover, the detected significantly different intensity of tree-ring eccentricity-based geomorphic signals in mass movement years and other years indicates the correctness of the dated mass movement events. In contrast, younger trees respond more readily through reaction wood (Šilhán, 2021a). Thus, the combination of mass movements recorded in both chronologies conveniently combines the advantages of both approaches, as already suggested by Corominas and Moya (1999) or Bollati et al. (2012). Conversely, a potential problem may be the inability to date with seasonal precision in the case of tree-ring eccentricity analysis (Braam et al., 1987; Šilhán, 2019; Wistuba et al., 2013), which theoretically may lead to inaccurate determination of the mass movement year if it occurs during the dormancy period. However, given the high proportion of synchronously determined mass movement years in both subchronologies, there does not appear to be a major effect on the resulting chronology here. The combination of both methodological approaches in a unique site with some of the oldest trees in the study region results in one of the longest chronologies of mass movements (see Šilhán, 2020). Thus, given the competent overlap of this chronology with meteorological data, this is the most robust overlay to date of both datasets with annual resolution in order to define potential

Table 2
Overview of the ten longest overlaps of instrumental meteorological data with tree-ring based chronologies of mass movements.

Order	Reference	Landslide type	Sample size	Chronology length	Overlaps with meteorological data	Data character	Data resolution
1	Šilhán et al., 2012	Rockslide	48	307	**132**	precipitation	monthly
2	Lopez Saez et al., 2013	Rotational and flow-like	759	114	**114**	precipitation	monthly
3	Wiktorowski et al., 2017	–	127	105	**102**	precipitation	annual
4	Šilhán et al., 2014	Shallow-medium deep	274	127	**101**	precipitation	monthly
5	Šilhán et al., 2013	Bedrock, translational	176	99	**99**	precipitation	monthly
6	Van den Eeckhaut et al., 2009	Deep-seated	33	80	**80**	precipitation	seasonal
7	Fantucci and Sorriso-Valvo, 1999	Shallow	24	175	**74**	precipitation	seasonal
8	Shroder, 1978	Boulder deposits	280	213	**73**	precipitation, temperature	annual
9	Fantucci and McCord, 1995	Flow-like	28	114	**69**	precipitation	seasonal
10	Wistuba et al., 2015	Complex	108	86	**64**	precipitation	daily

meteorological triggers of mass movements.

5.2. Meteorological triggers of mass movements

Many papers analysing landslides in the Western Outer Carpathians reported importance of extreme precipitation totals for their origin (e.g., Bíl et al., 2016; Krejčí et al., 2002; Pánek et al., 2011a, 2011b). But also a large amount of snow accumulated during the winter and its sudden melting in the spring months can be another factors triggering to the mass movement origin (e.g., Bíl et al., 2016; Bíl and Müller, 2008; Šilhán, 2012). The knowledge from these papers resulted in the use of nine different precipitation and snow characteristics (see Section 3.3) for the analysis of meteorological triggers for 23 mass movement years covered by instrumental meteorological data from the Mt. Kněhyně region (see Section 4.3). Less convenient situation was with description of detected mass movement years before 1900, for which both instrumental and documentary data were available, but not directly from that region. This was reflected in a low ranking of 19th-century mass movement years (see Table 1) which can be related to higher uncertainty in the used areal Moravian precipitation series (Brázdil et al., 2012a) during this century, calculated from the lower number of stations, moreover not located in the mountains, compared to the 20th–21st centuries. On the other hand, except 1835 all other mass movement years of the 19th century indicated rather wetter patterns in the Czech Lands witnessed by large amounts of snow with related snowmelt floods or long-lasting intense precipitation spells followed by rainy floods. Moreover, we may expect even much larger amounts of snow or higher precipitation totals particularly in the Moravskoslezské Beskydy Mts.

The observed influence of previous annual precipitation and, in part, snowmelt on mass process activity is consistent with the need for higher saturation of the landslide environment, which, in combination with subsequent short-term extreme precipitation events, will trigger the mass movement itself. This pattern of behaviour corresponds to moderate-deep landslides on slopes of moderate slope (Pánek et al., 2011a), as in the case of the study locality, where trees in the upper, rather flat, part of the landslide were analyzed also to eliminate the influence of creep movements on the resulting chronology.

5.3. Spatiotemporal context of landslides

Less settlement density in the Moravskoslezské Beskydy Mts. region complicates the possibility to find mass movement information from documentary evidence except of mass movements following July 1997 flood in Moravia and Silesia (Brázdil and Kirchner, 2007). From this reason it is not surprising, that newly involved Czech landslide database (CHILDA) by Bíl et al. (2021), based particularly on the Špůrek (1972) collection with a prevalence of recorded landslides from Bohemia, contains not any other documented cases for our selected mass movement years for the region analysed. The reported database has no landslide records for 12 of our 35 detected mass movement years (34.3 %) and in 5 years (14.3 %) it is only for one locality; 7 years (20 %) had recoded landslides from 2 to 5 places and the same number from 6 to 10 places. The year 1997 with 162 localities is followed by the years 1939 with 45 localities, 1926 with 28 localities and 1970 with 13 localities. These facts confirm importance of our study to identify further years and places of mass movements for the territory of the Czech Republic not known yet.

6. Conclusion

In this study, a series of mass movements over a quarter of a millennium was compiled using dendrogeomorphic methods from 57 old *P. abies* specimens. Detected mass movements involved mainly relaxed sandstone blocks and rocky colluvium forming the shallow subsurface of the deep-seated landslide. The resulting chronology was a unique combination of the results of two subchronologies, each based on different tree growth responses (reaction wood and tree-ring eccentricity). The resulting chronology of mass movements, combining the advantages of the two approaches used, could thus in the future represent a comprehensive effective tool for the compilation of long (several centuries; depending on the age of the trees) landslide chronologies. The obtained chronology was used in this case for the analysis of potential triggers. Due to the limited length of instrumental data from the nearest weather station, data from the wider region and documentary data were also used for this purpose, allowing a complete overlap with tree-ring based chronologies of mass movements. Reconstructed mass movement years were related to high annual precipitation totals in 1–3 years with triggering effects of extremely high totals during a few days as a dominant factor. Favourable snow patterns with high snow depths and sudden snowmelt could enhance in some mass movement years triggering precipitation effects. Means of all used precipitation characteristics in the set of mass movement years were statistically significantly higher than those in the set of other years.

Declaration of Competing Interest

The authors declare that they have no known competing financial interests or personal relationships that could have appeared to influence the work reported in this paper.

Data availability

Data will be made available on request.

Acknowledgements

KŠ and TP were supported by University of Ostrava project number SGS01/PřF/2022. RB and PZ were supported by the Ministry of Education, Youth and Sports of the Czech Republic for SustES – Adaptation strategies for sustainable ecosystem services and food security under adverse environmental conditions project ref. CZ.02.1.01/0.0/0.0/16_019/0000797. P. Štěpánek (Brno) is acknowledged for providing us with areal precipitation series for Moravia (1803–2020). We acknowledge Daniel Havlů for help with field sampling and Jan Lenart for providing data from geophysical measurements.

References

Bíl, M., Andrášik, R., Zahradníček, P., Kubeček, J., Sedoník, J., Štěpánek, P., 2016. Total water content thresholds for shallow landslides, Outer Western Carpathians. Landslides 13, 337–347. https://doi.org/10.1007/s10346-015-0570-9.

Bíl, M., Müller, I., 2008. The origin of shallow landslides in Moravia (Czech Republic) in the spring of 2006. Geomorphology 99, 246–253. https://doi.org/10.1016/j.geomorph.2007.11.004.

Bíl, M., Raška, P., Dolák, L., Kubeček, J., 2021. CHILDA – Czech Historical Landslide Database. Nat. Hazards Earth Syst. Sci. 21, 2581–2596. https://doi.org/10.5194/nhess-21-2581-2021.

Bollati, I., della Seta, M., Pelfini, M., del Monte, M., Fredi, P., Lupia Palmieri, E., 2012. Dendrochronological and geomorphological investigations to assess water erosion and mass wasting processes in the Apennines of Southern Tuscany (Italy). Catena (Amst.) 90, 1–17. https://doi.org/10.1016/j.catena.2011.11.005.

Braam, R.R., Weiss, E.E.J., Burrough, P.A., 1987. Spatial and temporal analysis of mass movement using dendrochronology. Catena (Amst.) 14, 573–584.

Brázdil, R., Bělínová, M., Dobrovolný, P., Mikšovský, J., Pišoft, P., Řezníčková, L., Štěpánek, P., Valášek, H., Zahradníček, P., 2012a. Temperature and Precipitation Fluctuations in the Czech Lands during the Instrumental Period. Masaryk University, Brno.

Brázdil, R., Demarée, G.R., Deutsch, M., Garnier, E., Kiss, A., Luterbacher, J., Macdonald, N., Rohr, C., Dobrovolný, P., Kolář, P., Chromá, K., 2010. European floods during the winter 1783/1784: scenarios of an extreme event during the 'Little Ice Age'. Theor. Appl. Climatol. 100, 163–189. https://doi.org/10.1007/s00704-009-0170-5.

Brázdil, R., Kirchner, K., 2007. Selected Natural Extremes and their Impacts in Moravia and Silesia. Masarykova univerzita, Český hydrometeorologický ústav. Ústav geoniky Akademie věd České republiky, v.v.i., Brno, Praha, Ostrava.

Brázdil, R., Pfister, C., Wanner, H., von Storch, H., Luterbacher, J., 2005. Historical climatology in Europe – the state of the art. Clim. Change 70, 363–430. https://doi.org/10.1007/s10584-005-5924-1.

Brázdil, R., Šilhán, K., Pánek, T., Dobrovolný, P., Kašičková, L., Tolasz, R., 2012b. The influence of meteorological factors on rockfall in the Moravskoslezské Beskydy Mts. Geografie 117, 1–20. 10.37040/geografie2012117010001.

Brázdil, R., Řezníčková, L., Valášek, H., Dolák, L., Kotyza, O., 2017. Climatic and other responses to the Lakagígar 1783 and Tambora 1815 volcanic eruptions in the Czech Lands. Geografie 122, 147–168. https://doi.org/10.37040/geografie201712202014.

Chitu, Z., Bogaard, T., Busuioc, A., Burcea, S., Sandric, I., Adler, M.-J., 2017. Identifying hydrological pre-conditions and rainfall triggers of slope failures at catchment scale for 2014 storm events in the Ialomita Subcarpathians, Romania. Landslides 14, 419–434. https://doi.org/10.1007/s10346-016-0740-4.

Cockburn, J.M.H., Vetta, M., Garver, J.I., 2016. Tree-ring evidence linking late twentieth century changes in precipitation to slope instability, central New York state, USA. Phys. Geogr. 37, 153–168. https://doi.org/10.1080/02723646.2016.1157741.

Cook, E.R., 1983. A time series analysis approach to tree-ring standardization. University of Arizona, USA, Tucson.

Corominas, J., Moya, J., 1999. Reconstructing recent landslide activity in relation to rainfall in the Llobregat River basin, Eastern Pyrenees, Spain. Geomorphology 30, 79–93. https://doi.org/10.1016/S0169-555X(99)00046-X.

Corona, C., Lopez Saez, J., Stoffel, M., 2014. Defining optimal sample size, sampling design and thresholds for dendrogeomorphic landslide reconstructions. Quat. Geochronol. 22, 72–84. https://doi.org/10.1016/j.quageo.2014.02.006.

Fabiánová, A., Chalupa, V., Šilhán, K., 2021. Dendrogeomorphic dating vs. low-magnitude landsliding. Quat. Geochronol. 62, 101150 https://doi.org/10.1016/j.quageo.2021.101150.

Fantucci, R., McCord, A., 1995. Reconstruction of landslide dynamic with dendrochronological methods. Dendrochronologia (Verona) 13, 43–58.

Fantucci, R., Sorriso-Valvo, M., 1999. Dendrogeomorphological analysis of a slope near Lago, Calabria (Italy). Geomorphology 30, 165–174. https://doi.org/10.1016/S0169-555X(99)00052-5.

Holmes, R., 1983. Computer-assisted quality control in tree-ring dating and measurement. Tree-Ring Bull. 43, 69–73.

Jakob, M., Holm, K., Lange, O., Schwab, J.W., 2006. Hydrometeorological thresholds for landslide initiation and forest operation shutdowns on the north coast of British Columbia. Landslides 3, 228–238. https://doi.org/10.1007/s10346-006-0044-1.

Khan, S., Kirschbaum, D.B., Stanley, T.A., Amatya, P.M., Emberson, R.A., 2022. Global landslide forecasting system for hazard assessment and situational awareness. Front. Earth Sci. (Lausanne) 10. https://doi.org/10.3389/feart.2022.878996.

Krejčí, O., Baroň, I., Bíl, M., Hubatka, F., Jurová, Z., Kirchner, K., 2002. Slope movements in the Flysch Carpathians of Eastern Czech Republic triggered by extreme rainfalls in 1997: a case study. Phys. Chem. Earth 27, 1567–1576. https://doi.org/10.1016/S1474-7065(02)00178-X.

Kříž, V., 1995. Laviny Hrubého Jeseníku, Králického Sněžníku a Moravskoslezských Beskyd. Acta Universitatis Ostraviensis 149, 69–86.

Lenart, J., Pánek, T., Dušek, R., 2014. Genesis, types and evolution of crevice-type caves in the flysch belt of the Western Carpathians (Czech Republic). Geomorphology 204, 459–476. https://doi.org/10.1016/j.geomorph.2013.08.025.

Lopez Saez, J., Corona, C., Stoffel, M., Astrade, L., Berger, F., Malet, J.P., 2012a. Dendrogeomorphic reconstruction of past landslide reactivation with seasonal precision: the Bois Noir landslide, southeast French Alps. Landslides 9, 189–203. https://doi.org/10.1007/s10346-011-0284-6.

Lopez Saez, J., Corona, C., Stoffel, M., Berger, F., 2013. Climate change increases frequency of shallow spring landslides in the French Alps. Geology 41, 619–622. https://doi.org/10.1130/G34098.1.

Menčík, E., Adamová, M., Dvořák, J., Dudek, A., Jetel, J., Jurková, A., Hanzlíková, E., Houša, V., Peslová, H., Rybářová, L., Šmíd, B., Šebesta, J., Tyráček, J., Vašíček, Z., 1983. Geologie Moravskoslezských Beskyd a Podbeskydské pahorkatiny. Ústřední ústav geologický, Praha.

Moran, P.A.P., 1950. Notes on continuous stochastic phenomena. Biometrika 37, 17–23.

Notti, D., Wrzesniak, A., Dematteis, N., Lollino, P., Fazio, N.L., Zucca, F., Giordan, D., 2021. A multidisciplinary investigation of deep-seated landslide reactivation triggered by an extreme rainfall event: a case study of the Monesi di Mendatica landslide, Ligurian Alps. Landslides 18, 2341–2365. https://doi.org/10.1007/s10346-021-01651-3.

Pánek, T., Hradecký, J., Minár, J., Hungr, O., Dušek, R., 2009. Late Holocene catastrophic slope collapse affected by deep-seated gravitational deformation in flysch: Ropice Mountain, Czech Republic. Geomorphology 103, 414–429. https://doi.org/10.1016/j.geomorph.2008.07.012.

Pánek, T., Šilhán, K., Tábořík, P., Hradecký, J., Smolková, V., Lenart, J., Brázdil, R., Kašičková, L., Pazdur, A., 2011a. Catastrophic slope failure and its origins: Case of the May 2010 Girová Mountain long-runout rockslide (Czech Republic). Geomorphology 130, 352–364. https://doi.org/10.1016/j.geomorph.2011.04.020.

Pánek, T., Tábořík, P., Klimeš, J., Komárková, V., Hradecký, J., Šťastný, M., 2011b. Deep-seated gravitational slope deformations in the highest parts of the Czech Flysch Carpathians: evolutionary model based on kinematic analysis, electrical imaging and trenching. Geomorphology 129. https://doi.org/10.1016/j.geomorph.2011.01.016.

Pánek, T., Břežný, M., Kapustová, V., Lenart, J., Chalupa, V., 2019. Large landslides and deep-seated gravitational slope deformations in the Czech Flysch Carpathians: New LiDAR-based inventory. Geomorphology 346, 106852. https://doi.org/10.1016/j.geomorph.2019.106852.

Pawelec, H., 2006. Origin and palaeoclimatic significance of the Pleistocene slope covers in the Cracow Upland, southern Poland. Geomorphology 74, 50–69. https://doi.org/10.1016/j.geomorph.2005.07.010.

Pawlik, Ł., Migoń, P., Owczarek, P., Kacprzak, A., 2013. Surface processes and interactions with forest vegetation on a steep mudstone slope, Stołowe Mountains, SW Poland. Catena (Amst.) 109, 203–216. https://doi.org/10.1016/j.catena.2013.03.011.

Raška, P., Klimeš, J., Dubišar, J., 2015. Using local archive sources to reconstruct historical landslide occurrence in selected urban regions of the Czech Republic: Examples from regions with different historical development. Land Degrad. Dev. 26 https://doi.org/10.1002/ldr.2192.

Saez, L., Jérôme, C., Stoffel, M., Schoeneich, P., Berger, F., 2012b. Probability maps of landslide reactivation derived from tree-ring records: Pra Bellon landslide, southern French Alps. Geomorphology 138, 189–202. https://doi.org/10.1016/j.geomorph.2011.08.034.

Shroder, J.F., 1978. Dendrogeomorphological analysis of mass movement on Table Cliffs Plateau, Utah. Quat. Res. 9, 168–185. https://doi.org/10.1016/0033-5894(78)90065-0.

Šilhán, K., 2012. Dendrogeomorphological analysis of the evolution of slope processes on flysch rocks (Vsetínské vrchy Mts; Czech Republic). Carpathian J. Earth Environ. Sci. 7, 39–49.

Šilhán, K., 2016. How different are the results acquired from mathematical and subjective methods in dendrogeomorphology? Insights from landslide movements. Geomorphology 253, 189–198. https://doi.org/10.1016/j.geomorph.2015.10.012.

Šilhán, K., 2019. Tree-ring eccentricity in the dendrogeomorphic analysis of landslides – a comparative study. Catena (Amst.) 174, 1–10. https://doi.org/10.1016/j.catena.2018.11.002.

Šilhán, K., 2020. Dendrogeomorphology of landslides: principles, results and perspectives. Landslides 17, 2421–2441. https://doi.org/10.1007/s10346-020-01397-4.

Šilhán, K., 2021a. The age-dependent sensitivity of *Picea abies* (L.) H. Karst. to landslide movements. Sci. Total Environ. 776 https://doi.org/10.1016/j.scitotenv.2021.145933.

Šilhán, K., 2021b. Dendrogeomorphology of different landslide types: a review. Forests. https://doi.org/10.3390/f12030261.

Šilhán, K., 2023. Historical activity of debris flows in the medium-high mountains: regional reconstruction using dendrogeomorphic approach. Sci. Total Environ. 856, 159248 https://doi.org/10.1016/j.scitotenv.2022.159248.

Šilhán, K., Brázdil, R., Pánek, T., Dobrovolný, P., Kašičková, L., Tolasz, R., Turský, O., Václavek, M., 2011. Evaluation of meteorological controls of reconstructed rockfall activity in the Czech Flysch Carpathians. Earth Surf. Proc. Land. 36, 1898–1909. https://doi.org/10.1002/esp.2211.

Šilhán, K., Pánek, T., Hradecký, J., 2012. Tree-ring analysis in the reconstruction of slope instabilities associated with earthquakes and precipitation (the Crimean Mountains, Ukraine). Geomorphology 173–174, 174–184. https://doi.org/10.1016/j.geomorph.2012.06.010.

Šilhán, K., Pánek, T., Dušek, R., Havlů, D., Brázdil, R., Kašičková, L., Hradecký, J., 2013. The dating of bedrock landslide reactivations using dendrogeomorphic techniques: The Mazák landslide, Outer Western Carpathians (Czech Republic). Catena (Amst.) 104, 1–13. https://doi.org/10.1016/j.catena.2012.12.010.

Šilhán, K., Pánek, T., Turský, O., Brázdil, R., Klimeš, J., Kašičková, L., 2014. Spatio-temporal patterns of recurrent slope instabilities affecting undercut slopes in flysch: a dendrogeomorphic approach using broad-leaved trees. Geomorphology 213, 240–254. https://doi.org/10.1016/j.geomorph.2014.01.016.

Šilhán, K., Pánek, T., Škarpich, V., 2022a. Diversification of landslide areas as a means for reducing noise in dendrogeomorphic dating. Quat. Geochronol. 72, 101362 https://doi.org/10.1016/j.quageo.2022.101362.

Šilhán, K., Pánek, T., Škarpich, V., Břežný, M., Chalupa, V., 2022b. Specifics of slope movements on slopes with contrasting structural conditions: evidence from tree-ring records. Geomorphology 415, 108425. https://doi.org/10.1016/j.geomorph.2022.108425.

Šilhán, K., Stoffel, M., 2015. Impacts of age-dependent tree sensitivity and dating approaches on dendrogeomorphic time series of landslides. Geomorphology 236, 34–43. https://doi.org/10.1016/j.geomorph.2015.02.003.

Špůrek, M., 1972. Historical catalogue of slide phenomena. Stud. Geogr. 19, 1–179.

Stefanini, M.C., 2004. Spatio-temporal analysis of a complex landslide in the Northern Apennines (Italy) by means of dendrochronology. Geomorphology 63, 191–202. https://doi.org/10.1016/j.geomorph.2004.04.003.

Stemberk, J., Hartvich, F., Blahůt, J., Rybář, J., Krejčí, O., 2017. Tectonic strain changes affecting the development of deep seated gravitational slope deformations in the Bohemian Massif and Outer Western Carpathians. Geomorphology 289, 3–17.

Stoffel, M., Beniston, M., 2006. On the incidence of debris flows from the early Little Ice Age to a future greenhouse climate: a case study from the Swiss Alps. Geophys. Res. Lett. 33, 1–4. https://doi.org/10.1029/2006GL026805.

Stoffel, M., Bollschweiler, M., 2008. Tree-ring analysis in natural hazards research - an overview. Nat. Hazards Earth Syst. Sci. 8, 187–202. https://doi.org/10.5194/nhess-8-187-2008.

Stoffel, M., Butler, D.R., Corona, C., 2013. Mass movements and tree rings: A guide to dendrogeomorphic field sampling and dating. Geomorphology 200, 106–120. https://doi.org/10.1016/j.geomorph.2012.12.017.

Stoffel, M., Corona, C., 2014. Dendroecological dating of geomorphic disturbance in trees. Tree-Ring Res. 70, 3–20. https://doi.org/10.3959/1536-1098-70.1.3.

Tolasz, R., Míková, T., Valeriánová, A., Voženílek, V., 2007. Climate Atlas of Czechia.Český hydrometeorologický ústav, Palackého univerzita, Praha, Olomouc.

V.I.A.S., 2005. Vienna Institute of Archaeological Science, Time Table. Installation and instruction manual.

van den Eeckhaut, M., Muys, B., van Loy, K., Poesen, J., Beeckman, H., 2009. Evidence for repeated re-activation of old landslides under forest. Earth Surf. Proc. Land. 34, 352–365. https://doi.org/10.1002/esp.1727.

Wagner, J., Demek, J., Stráník, Z., 1990. Caves in the Moravskoslezské Beskydy Mts. and their surroundings. Česká speleologická společnost, Bohumín.

Westing, A.H., 1965. Formation and function of compression wood in gymnosperms II. Bot. Rev. 34, 51–78.

Wiktorowski, D., Krąpiec, M., Lutka, M., 2017. Dendrogeomorphological analysis of landslide activity along the planned S-69 road in the Węgierska Górka municipality (Beskid Śląski Mountains, S Poland). Geol. Geophys. Environ. 43, 139. https://doi.org/10.7494/geol.2017.43.2.139.

Wistuba, M., Malik, I., Gärtner, H., Kojs, P., Owczarek, P., 2013. Application of eccentric growth of trees as a tool for landslide analyses: the example of *Picea abies* Karst. in the Carpathian and Sudeten Mountains (Central Europe). Catena (Amst.) 111, 41–55. https://doi.org/10.1016/j.catena.2013.06.027.

Wistuba, M., Malik, I., Wójcicki, K., Michałowicz, P., 2015. Coupling between landslides and eroding stream channels reconstructed from spruce tree rings (examples from the Carpathians and Sudetes - Central Europe). Earth Surf. Proc. Land. 40, 293–312. https://doi.org/10.1002/esp.3632.

Wistuba, M., Gorczyca, E., Malik, I., 2021a. Inferring precipitation thresholds of landslide activity from long-term dendrochronological and precipitation data: case study on the unstable slope at Karpenciny, Poland. Eng. Geol. 294, 106398 https://doi.org/10.1016/j.enggeo.2021.106398.

Wistuba, M., Malik, I., Gorczyca, E., Ślęzak, A., 2021b. Establishing regimes of landslide activity – analysis of landslide triggers over the previous seven decades (Western Carpathians, Poland). Catena (Amst.) 196, 104888. https://doi.org/10.1016/j.catena.2020.104888.

Xian, Y., Wei, X., Zhou, H., Chen, N., Liu, Y., Liu, F., Sun, H., 2022. Snowmelt-triggered reactivation of a loess landslide in Yili, Xinjiang, China: mode and mechanism. Landslides 19, 1843–1860. https://doi.org/10.1007/s10346-022-01879-7.

Zhang, Y., Stoffel, M., Liang, E., Guillet, S., Shao, X., 2019. Centennial-scale process activity in a complex landslide body in the Qilian Mountains, northeast Tibetan Plateau, China. Catena (Amst.) 179, 29–38.